# Peak shaving through real-time scheduling of household appliances

Davide Caprino, Marco L. Della Vedova, Tullio Facchinetti*

*Dept. of Electrical, Computer and Biomedical Engineering*
*University of Pavia*
*via Ferrata 1 – 27100 Pavia, Italy*

**Abstract**

The problem of limiting the peak load of the power consumed by a set of electric loads has been largely addressed in over 5 decades of research on power systems. The motivation of such attention arises from the benefits that a smoother load profile brings to the management of power systems.

This paper illustrates an approach to the peak shaving problem that leverages the real-time scheduling discipline to coordinate the activation/deactivation of a set of loads. The real-time scheduling is an active research topic in the field of computing systems. The innovative idea proposed in this paper is to apply existing real-time scheduling algorithms and analysis methods to the management of power loads. This solution requires an adequate modeling of considered devices in order to derive a representation in terms of timing parameters. The modeling approach enables the handling of a set of heterogeneous loads in a coordinated manner. In particular, this paper focuses on the modeling and management of household appliances. For this purpose, a set of the most common appliances is modeled and their activation is controlled by the proposed scheduling policy. Realistic assumptions are made on the daily usage of each device. The derived results show an effective and predicable reduction of the peak load while guaranteeing the user comfort associated with the load operation. The peak load of a single apartment is reduced by the 8% in the average case and by the 41% w.r.t. the worst-case. Considering the coalition of several apartments, the scheduling approach achieves a peak load reduction up to 46%.

*Keywords:* real-time, scheduling, modeling, peak shaving, home energy management, demand-side management, electric load management, virtual electricity consumer

## 1. Introduction

The problem of limiting the peak of power consumed by a set of electric loads has been widely studied in the field of power systems [1]. The advantage of achieving a limited peak load are both on the energy provider and user side. The coordination of electric loads is often addressed in the context of *smart grids* under the so-called Demand-Side Management (DSM) [2]. The DSM addresses techniques targeted to the regulation of the demanded electric power.

This paper describes a method to coordinate a set of electric loads to limit the peak load of power usage. The proposed method leverages the real-time scheduling discipline to coordinate the activation/deactivation of the load set. Real-time scheduling is an active research field in the computer science domain, where it is studied to manage the concurrent execution of processing tasks on a set of processors under timing constraints [3]. The innovative idea proposed in this paper is to adapt some existing real-

*Corresponding author
*Email addresses:* davide.caprino01@ateneopv.it (Davide Caprino), marco.dellavedova@unipv.it (Marco L. Della Vedova), tullio.facchinetti@unipv.it (Tullio Facchinetti)

time scheduling and analysis methods to coordinate the activation of activations power loads. This solution requires an adequate modeling of the considered loads to derive a representation in terms of timing parameters. Suitable parameters can be found applying the so-called Real-Time Physical System (RTPS) model [4]. The most remarkable features of a power load management based on real-time scheduling algorithms are:

- predictability: the behavior of a real-time scheduling pattern is a-priori guaranteed in a mathematically strong form [3];
- robustness: real-time scheduling algorithms are concerned with worst-case working conditions [3];
- reusability: there are several modeling and control methodologies that can be adapted and applied to the load management [5];
- automatization: the derivation of load priorities is based on the characteristics of both the load and the underlying physical process, without the need of the empirical intervention of a system designer [6];
- scalability: thanks to low-complexity algorithms, large sets of heterogeneous loads can be effectively managed and analyzed [7].

Although the proposed method can handle a set of heterogeneous loads, including industrial loads [8, 9], this paper focuses on the modeling and the management of household appliances. Figure 1 depicts a Home Energy Management (HEM) infrastructure that allows to manage the appliances of several houses/apartments in a coordinated manner. This aggregated organization is known as *coalition*, and the set of users are seen as a Virtual Electricity Consumer [10].

For this purpose, a set of the most common appliances is modeled and real-time scheduling algorithms are applied to their coordination. The considered loads are classified as *time-triggered* (TT) or *event-triggered* (ET) loads. A TT load generated a periodic sequence of activation requests. The TT loads considered in this paper are refrigerators and Heating, Ventilating and Air Conditioning (HVAC) systems. On the other hand, the activation of ET loads is triggered by the user. In this case, the automatic coordination system schedules the load activity within a given time interval. The considered ET loads are washing machines, dishwashers, and electric ovens. The type of loads to model has been selected considering two parameters: its penetration rate, i.e., the percentage of the population that purchased the appliance, and its controllability. The former allows to neglect those appliances that are not widely spread. Only appliances having a penetration rate above 50% have been considered. The penetration rate has been evaluated on the Italian market, based on the information reported in [11]. The controllability refers to those loads that can be suitably managed by a centralized controller, i.e., loads that can be freely turned on/off without affecting the user comfort. For this reason, non-controllable loads such as televisions and the lighting systems have been excluded.

For each considered load a simple but accurate thermodynamic model has been derived. The model is used to determine the values of timing parameters required to perform an active control using real-time scheduling techniques. The derived profiles have been validated against real measured ones. The sources of measured profiles are [12], a report developed in collaboration with the European Committee of Domestic Equipment Manufacturers (CECED), and [13]. Realistic assumptions are made on the daily usage of each load.

The derived results show an effective and predictable reduction of the peak load while guaranteeing the user comfort associated with the load operation. In particular, when the proposed approach is applied in the context of a single apartment, simulation results show that the peak load can be reduced from 8% up to 41%, for some load ac-

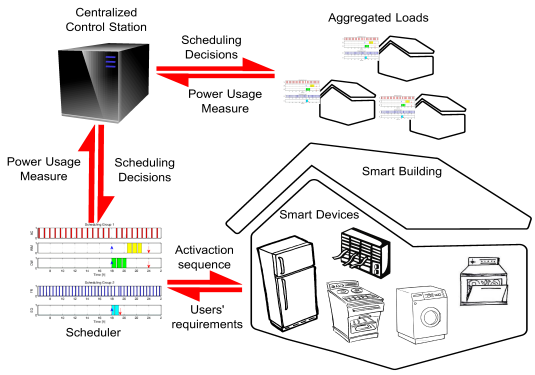


Figure 1: The Home Energy Management system based on real-time control techniques.

tivation patterns. Moreover, when a group of users forms a coalition the benefits increase: the reduction is up to the 46% w.r.t. worst-case conditions.

### *1.1. Paper organization*

The paper is organized as follows. Section 2 provides a short introduction to the state of the art of electric load management. In Section 3 the physical models of the processes controlled by the considered electric devices are presented. Section 4 illustrates the proposed Home Energy Management strategy, describing the adopted algorithms and the timing characterization of loads. Since some of the evaluated appliances, like washing machines and ovens, are activated by the user, considerations on the user behavior are reported in Section 5. In Section 6, an example of application is provided on a single apartment, while Section 7 derives simulation results on a coalition. Finally, Section 8 states our conclusions.

## 2. Related works

This section focuses on existing modeling and coordination approaches targeted to peak load management.

Several papers propose physically based load models of electric loads and appliances [14, 15, 16]. However, such models are either uselessly detailed for our purposes or they simply neglect loads that are considered in this paper. We have tailored the complexity of our proposed models to address the modeling in terms of timing parameters.

Over the decades, approaches based on optimization techniques as linear programming [17] and linear control methods [18] have been proposed. Another class of approaches is based on artificial intelligence techniques, such as neural networks [19], self organizing agents [20], fuzzy logic [21, 22], and expert systems [23]. Those methods do not provide any predictable forecasting on the achievable peak load. Some works address the management of distributed energy generation, i.e., from renewable sources [24]. Other ones target the cost optimization associated with the peak load management [25]. Finally, some works only address the modeling of loads, but do not propose a specific method to reduce the peak load [26].

Recently, the green scheduling has been proposed in [27]. It addresses the peak reduction problem by scheduling multiple interacting control systems within a constrained peak demand envelope, while ensuring that safety and operational conditions are guaranteed. This solution efficiently deals with the scheduling periodic loads. However, the approach has been tested on small-scale systems. Moreover, the model does not consider ET loads, but only thermal loads are simulated. Finally, the problem of limiting the frequency of load interruption is not investigated.

In [28], the authors use an approach similar to the one adopted in this paper. First, they define a physical model of many household appliances. Then, they leverage the model to test their Home Energy Management algorithm [29] on the experimental set. Unlike our proposal, however, the referred method is based on the manual specification of load priorities. E.g., the user or a system designer needs to explicitly set the priorities of all loads. This method has scalability issues when the number of loads increases. Although our approach is also based on the assignment of load priorities, the real-time scheduling algorithm provides an automatic method for the priority assignment. The selection of the loads to activate is done, in fact, by

dynamically assigning the priority to every load based on its timing parameters. At any given instant, the highest priority loads are activated. The assignment of priorities is automatically performed by the scheduler, as done in real-time computing systems. Moreover, timing parameters are determined on the basis of physical characteristics and constraints of the underlying controlled process.

The peak shaving method based on real-time scheduling has been firstly presented in [30, 31], focusing on physical systems modeled as affine dynamic systems. The term *Real-Time Physical System* was introduced in [32], where systems with affine dynamics have been studied. Further studies have been carried out in [4, 33], considering constraints on state variable variations and modeling errors. In [7], the method is applied to a large set of HVAC loads. In some previous works, real-time scheduling is also applied to the management of industrial loads, such as air compressors [9] and manufacturing processes [8].

## 3. Modeling the physical systems

This section describes the physical model of the considered loads. The loads are divided into time-triggered (TT) and event-triggered (ET) loads. While the former loads require an activation on a regular basis, ET loads are activated upon user request. It is worth to outline that, although a TT load requires to be activated periodically, the activation can be delayed by the scheduling algorithm to avoid unnecessary simultaneous activations. Nevertheless, the delay is enforced while achieving the operational requirements of the load.

For all loads, the operating state is described by the activation function $s_i(t)$ in accordance with (1):

$$s_i(t) = \begin{cases} 0 & \text{load is inactive} \\ 1 & \text{load is active} \end{cases} \tag{1}$$

When the load is active, it absorbs a nominal power $P_i$; no power otherwise.

### 3.1. Time-triggered loads

The operating state of the $i$-th TT load is established by the control system on the basis of the value assumed by a state variable $X_i(t)$ associated with the load. TT loads are refrigerators and HVAC systems, thus $X_i(t)$ represents the internal temperature and the room temperature, respectively. The state variable must be bounded in a user-defined working range $[\overline{X}_i - \Delta_i, \overline{X}_i + \Delta_i]$.

The behavior of the state variable is described by a dynamical system model of the underlying physical process:

$$\frac{\mathrm{d}X_i(t)}{\mathrm{d}t} = f^{s_i(t)} = \begin{cases} -\alpha_i^{\mathrm{on}} & \text{if } s_i(t) = 1 \\ +\alpha_i^{\mathrm{off}} & \text{if } s_i(t) = 0 \end{cases} \tag{2}$$

In (2), $\alpha_i^{\mathrm{on}} > 0$ and $\alpha_i^{\mathrm{off}} > 0$ are constant values representing respectively the decreasing and increasing slopes of the state variable. The choice of a negative slope associated with the activation state is made considering the so-called *cold appliances*, whose goal is to reduce the system temperature. This assumption does not affect the generality of the proposed approach, since similar arguments apply to *heating appliances*.

Equation (2) defines a linear variation of the state variable. Nonetheless, such kind of variation can suitably approximate more articulated systems, e.g., having exponential behavior. This is a tolerable approximation when working ranges associated with the variation of the state variable are sufficiently narrow with respect to system dynamics determined by the time constants [34, 35, 36].

Since all the considered loads are characterized by on/off operations, their load profiles can be deduced from their dynamics behavior and from their power consumption in each state of activation. For both the analyzed TT loads the state variable is the temperature. Therefore, to derive their activation/deactivation timing behavior, i.e. the values of $\alpha_i^{\mathrm{on}}$ and $\alpha_i^{\mathrm{off}}$, it is necessary to provide their thermodynamic model.

Considering the first law of thermodynamics $\Delta U = Q$, where $\Delta U = C\Delta T$ is the internal energy variation and $Q$ is

the exchanged heat, and considering the timing derivative, it holds:

$$C_i \dot{T}_i = \dot{Q}_i \tag{3}$$

where $C_i$ is the heat capacity of the system. The heat transmission $\dot{Q}_i$ accounts for radiation, conduction and convection heat losses. Moreover, when the load is active, $\dot{Q}_i$ also includes the heat power $P_i$ of the considered load:

$$\dot{Q}_i = -P_i + \dot{Q}_i^{\text{losses}} \tag{4}$$

To determine the heat losses, three types of heat transmission have been considered.

First, the heat losses for steady state conduction are calculated. Thermal conductivities, as well as internal and external temperatures, are considered as constants for the selected working conditions. Under these assumptions, the Fourier Conduction Law can be simplified as:

$$\dot{Q}_{\text{cond}} = \frac{A \cdot (T^e - T^{int})}{\sum_{k=1}^{n} \frac{s_k}{\lambda_k}} \tag{5}$$

where $A$ is the transmission area, $T^{\text{int}}$ is the internal load temperature, $T^e$ is the external temperature, $\lambda_k$ and $s_k$ represent respectively the thermal conductivity and the thickness of the $k$-th layer of the considered surface.

Second, despite the complexity of the convection phenomenon, the rate of convection heat transfer could be conveniently expressed by the Newton's law as:

$$\dot{Q}_{\text{conv}} = A \cdot h_c \cdot (T^e - T^{int}) \tag{6}$$

The convective heat transfer coefficient $h_c$ depends on the type of media, gas or liquid, from flow properties such as velocity, viscosity and other flow- and temperature-dependent properties.

Last, the heat radiative transfer could be expressed considering the Stefan-Boltzmann's law in its linearized form:

$$\dot{Q}_{\text{rad}} = A \cdot h_r \cdot (T^e - T^{int}) \tag{7}$$

The radiative heat coefficient is $h_r = 4\epsilon\sigma T_m^3$, where $\epsilon$ is the emissivity of the considered material, which takes into account the ability of a surface to emit energy by radiation. The coefficient $\sigma$ is a constant value known as Stefan-Boltzmann coefficient. $T_m$ is the average of $T_{int}$ and $T_e$.

Considering that conduction and radiation both depend on the surface properties, the coefficient $h$ can be introduced to take in account both effects: $h = h_c + h_v$. $h$ is said *liminar coefficient*. It follows that:

$$\dot{Q}_{\text{liminar}} = \frac{(T^e - T^{int})}{R^{\text{liminar}}} \tag{8}$$

where $R^{\text{liminar}}$ is the thermal convection and radiation resistance defined as:

$$R^{\text{liminar}} = \frac{1}{h \cdot A} \tag{9}$$

Considering (5), (6), (7) and (8), the following relationship holds:

$$\dot{Q}_{\text{losses}} = \dot{Q}_{\text{cond}} + \dot{Q}_{\text{liminar}} = \frac{T^e - T^{int}}{R^{\text{cond}} + R^{\text{liminar}}} \tag{10}$$

where $R^{\text{cond}}$ is the thermal conduction resistance:

$$R^{\text{cond}} = \frac{A}{\sum_{k=1}^{n} \frac{s_k}{\lambda_k}} \tag{11}$$

Therefore it follows from (3), (4) and (10):

$$\alpha_i^{\text{on}} = \frac{1}{C_i}\left(P_i - \frac{T^e - T^{\text{int}}}{R^{\text{cond}} + R^{\text{conv}}}\right) \tag{12a}$$

$$\alpha_i^{\text{off}} = \frac{1}{C_i}\left(\frac{T^e - T^{\text{int}}}{R^{\text{cond}} + R^{\text{conv}}}\right) \tag{12b}$$

Taking into account the refrigerator, its heat capacity $C_i$ depends on the content and its structural materials. Therefore, the thermal behavior of the refrigerator has been derived by considering the thermal characteristics of some possible content of the fridge. In details, the set of products in the fridge is depicted in Tab. 1. The total thermal capacity is obtained by combining the thermal capacities of contained food and fridge structure: $C_i = C_{str} + \sum_k m_k c_k$.

Figures 2 and 3 respectively show the temperature and power profiles of the modeled refrigerator and HVAC units.

### *3.2. Event-triggered loads*

The operating state of ET loads depends on the specific functionality of the device, which often – although

| Food | specific heat [kJ/(kgK)] | full [kg] | half [kg] | empty [kg] |
|---|---|---|---|---|
| water | 4.18 | 4 | 2 | 0 |
| milk | 3.85 | 1 | 0.5 | 0 |
| fruit | 3.34 | 2 | 1 | 0 |
| onion | 3.59 | 0.5 | 0.25 | 0 |
| ham | 3.05 | 0.2 | 0.1 | 0 |
| bread | 2.72 | 0.3 | 0.15 | 0 |
| beef | 3.43 | 0.4 | 0.2 | 0 |
| cheese | 2.09 | 0.5 | 0.25 | 0 |
| artichokes | 3.89 | 0.3 | 0.15 | 0 |
| cucumbers | 4.1 | 0.4 | 0.2 | 0 |
| thermal capacity [kJ/K] | - | 45.92 | 22.96 | 0 |

Table 1: List of some foods that may be contained into the refrigerator with their specific heat $c_k$ and mass $m_k$ in three cases: (a) full, (b) half and (c) empty.

not always – is affected by the behavior of a state variable. For instance, the centrifuge of a washing machine has a pre-defined duration that depends on the type of washing cycle, which is not related to a state variable variation. Nevertheless, the behavior of the internal temperature for the considered ET loads (washing machine, dishwasher and electric oven) plays an important role in the evaluation of their power absorption profiles. Therefore, this section proposes a thermodynamic model of such loads. The model is built by including the result provided by Equation (10) into Equation (4).

### *3.2.1. Washing machine*

The profile of electric usage of the washing machine is determined by the absorption and duration of each phase of the working cycle. The operating phase may significantly change among different models. The derived considerations refer to a typical class A 40°C washing cycle [37]. The washing cycle includes the following steps:

1. The required water is loaded during the first 800 seconds by the circulation pump and the drum is put in slow rotation to uniformly distribute the detergent;
2. In the heating phase, the water temperature is raised up to the set-point value;
3. The soaking phase regulates the drum rotation to optimize the washing process;
4. The centrifuge phase reduces the water content of dresses through fast drum rotations.

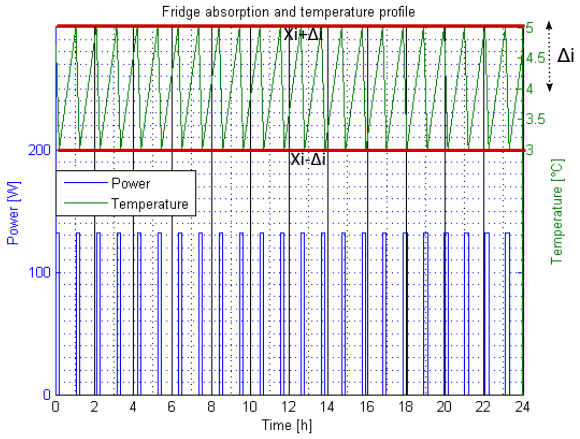


Figure 2: Power and temperature profiles of a full refrigerator. The set-point of the temperature is $4°\text{C} \pm 1$. The consumed power is 132 W.

Figure 4 shows the load absorption profile determined by the chosen working cycle and temperature profile. The peak of power usage is during the water heating phase. This is the only step that requires the control of the system temperature. In this phase, a thermal resistance is powered until the water reaches the set-point temperature. To determine the rate of temperature change, and consequently the water heating duration, Equation (12) must be applied. Considering the structural material of the washing machine, it is possible to determine the thermal conduction, convection resistances and the thermal capacity. The external temperature $T^{\text{e}}$ is the room temperature. It is considered constant, equal to 20°C. The temperature $T^{\text{i}}$ is the washing cycle set-point, equal to 40°C.

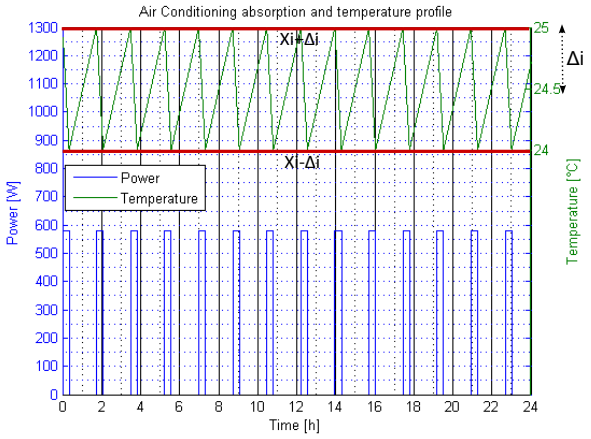


Figure 3: Power and temperature profiles of a HVAC unit. It is obtained considering a cooling system sized for a 26 $m^2$ room. The space cooling system is supposed to work continuously all day long. The set-point temperature is $24.5°C \pm 0.5$.

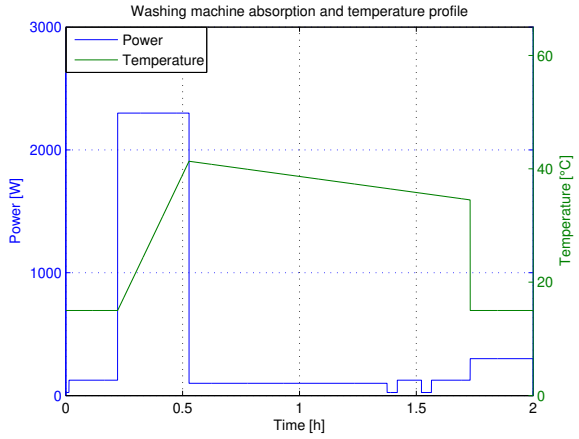


Figure 4: Power and temperature profiles of the modeled washing machine. This profile considers a 40°C washing cycle for a peak power of 2300 W.

### *3.2.2. Dishwasher*

Similarly to the approach adopted for the washing machine, the peak load generated by a dishwasher occurs during the water heating phases. In this case, the water is heated twice: the first time to prepare the water for the washing phase and then for the rinsing phase.

Figure 5 shows the absorption and temperature profiles of a typical class A dishwasher washing cycle calculated by means of Equation (12). The highest reached temperature $T^e$ is 62.5°C. This value is not controlled between the two heating phases. The thermal capacity, the thermal conduction and convection resistances are calculated considering the structural materials of a typical dishwashers. The room temperature $T^i$ is considered constant and equal to 20°C.

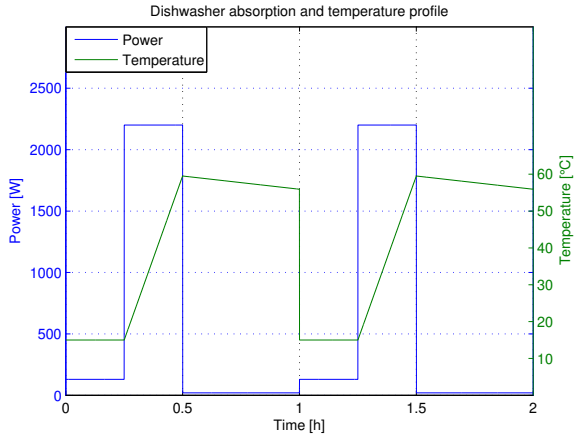


Figure 5: The power and temperature profile of a dishwasher. A peak power of 2200 W for each working cycle.

### *3.2.3. Electric Oven*

The state variable of an electric oven is its internal temperature. Unlike other ET loads, its value is kept under control during all the operation cycle. However, its behavior heavily depends on the type and amount of food that is loaded. In the proposed simulation, a cooking cycle of 1 hour for 1.5 Kg of potatoes has been considered. Under this assumption, the thermodynamic model presented in Section 3.1 has been used to determine the temperature rate. The power absorption profile is thus derived from such information. In particular, considering the structural materials and the chosen cooking cycle, it is possible to determine the thermal capacity, the conduction and convection resistances. Applying Equation (12) for the set-point temperature $T^e = 180°C$ and the constant room temperature $T^i = 20°C$, the temperature rate was calculated. Consequently, the timing of activations was derived. Once

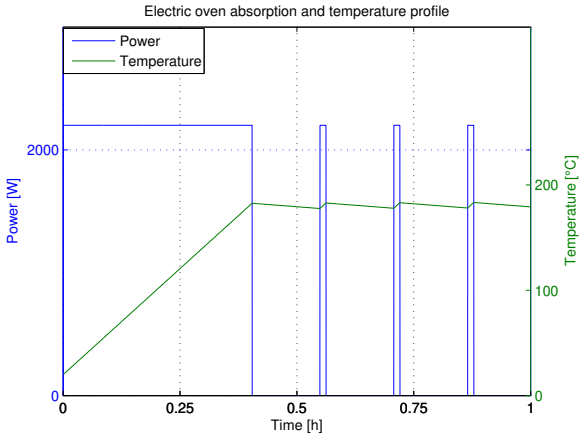


Figure 6: Power and temperature profiles of the electric oven. An electric oven working cycle with a peak power of 2200 W and a set-point temperature of 180°C is considered.

the set-point temperature is reached, the oven generates a periodic activation/deactivation pattern (see Figure 6), causing the temperature to range from 170°C to 180°C. Therefore, considering the operation in steady state conditions, the technique described in Section 3.1 could be applied. However, in this paper we made the pessimistic assumption that the activation of the electric oven is purely event-triggered, consuming the peak power for the whole working period. The exploitation of this peculiar behavior will be studied in a future work to apply the load scheduling technique during the periodic phase of the oven.

## 4. The Home Energy Management strategy

The HEM strategy consists in the application of a real-time scheduling algorithm to limit the peak power consumption of the considered residential electric loads. The scheduling algorithm is computed by the so-called *scheduler*, which acts as a centralized system controller. The scheduler generates the activation function $s_i$ (see eq. (1)) for each electric load. Since the $i$-th device consumes a $P_i$ amount of electric power if active and no power otherwise, the peak load $P^{\max}$ of a system made by $n$ loads is the maximum value of the following function $w(t)$:

$$w(t) = \sum_{i=1}^{n} P_i s_i(t) \tag{13}$$

The objective of the scheduling algorithm is to generate an activation pattern that reduces the peak load $P^{\max}$.

### *4.1. Timing characterization*

The use of a real-time scheduling algorithm requires to model the activation of each load in terms of real-time parameters. TT and ET loads are modeled by different sets of parameters. The meaning of these parameters is described in this section.

#### *4.1.1. Time-triggered loads*

The $i$-th TT load is described by the tuple $(T_i, D_i, C_i)$, where:

- $T_i$ is the *period* of activation;
- $D_i \leq T_i$ is the *relative deadline* of the load;
- $C_i \leq D_i$ is the duration of the *activation time* during each period;

According to these parameters, the schedule of a TT load is made by a sequence of activation requests. The $k$-th request happens at time $r_{i,k} = kT_i$, with $k = 0, 1, \ldots$. The term $r_{i,k}$ is said *request time*. After a request, the scheduler is responsible to switch on the load for $C_i$ time units within the $[r_{i,k}, d_{i,k}]$ time interval. The $d_{i,k} = r_{i,k} + D_i$ time instant is said *absolute deadline*, and it represents the latest instant to complete the execution of the $k$-th request. Notice that, while the absolute deadline refers to a single activation request, the relative deadline is a property of the load.

The activity-time of a load can be delayed within each period. Therefore, the activation may not necessarily begin at time $r_{i,k}$. Moreover, the activity of a load can be temporarily stopped to activate a more urgent load, and resumed later. In the real-time scheduling jargon, this event is said *preemption*.

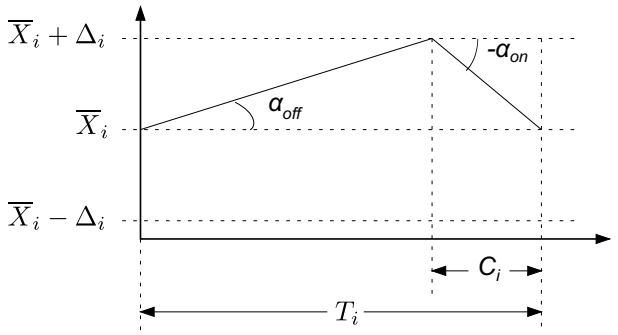


Figure 7: Geometric representation of the relation between physical and timing parameters for a "cold" appliance.

A very useful figure related to TT loads is the so-called *utilization*. The utilization $U_i$ of the $i$-th load is defined as

$$U_i \doteq \frac{C_i}{T_i}$$

It represents the percentage of activity time of the load. The total utilization of the load set is

$$U^{\text{tot}} = \sum_{i=1}^{n} U_i$$

Considering the dynamic model expressed by (2), in absence of perturbations, modeling errors and approximations, the results in [33] can be used to derive the following expressions for the timing parameters:

$$\begin{cases} T_i = \Delta_i \dfrac{\alpha_i^{\text{on}} + \alpha_i^{\text{off}}}{\alpha_i^{\text{on}} \alpha_i^{\text{off}}} \\ C_i = \dfrac{\Delta_i}{\alpha_i^{\text{on}}} \end{cases} \tag{14}$$

In [33] it is proved that this assignment of timing parameters guarantees the state variable to remain within the working range in every condition, i.e., this property holds for every valid schedule, regardless activation delays and preemptions. Figure 7 graphically shows the relationship between physical and timing parameters.

In a more realistic case, modeling errors, disturbances and approximations can not be neglected. Model inaccuracies are determined by several factors: oversimplification of the physical model, rounding in calculations, noise or interference on the physical system. For example, the proposed air-cooling model approximates the external temperature to be constant during the whole working time. In [33], a closed-loop approach is proposed to cope with such approximations. The closed-loop approach consists in adapting the value of the activation time $C_i$ at every request time in order to balance the effect of the disturbance. For this purpose, a measure of the value of the state variable in correspondence to the request time is required. The detected gap between measured value $\hat{X}_i(t)$ and expected value $\bar{X}_i$ is used to adjust $C_{i,k}$, which will be valid for the next time period $[r_{i,k}, r_{i,k} + D_i]$:

$$C_{i,k} = \frac{\Delta_i}{\alpha_i^{\text{on}}} + \frac{\hat{X}_i(t) - \bar{X}_i}{\alpha_i^{\text{on}} + \alpha_i^{\text{off}}} \tag{15}$$

In this case, the load utilization is defined using the maximum possible $C_{i,k}$. Its value can be calculated considering bounded disturbance (see [33] for details).

#### *4.1.2. Event-triggered loads*

The $i$-th ET load is described by the tuple ($r_i$, $D_i$, $C_i$), where:

- $r_i$ is the *request time* of the load, which is set by the user when the appliance is turned ON;
- $D_i$ is the *relative deadline*; a load activation at time $r_i$ is required to complete its execution before the absolute deadline $d_i = r_i + D_i$;
- $C_i \leq D_i$ is the maximum duration of the *activation time*;

The assumption made in this paper is that the user can explicitly set the deadline for the process associated with the load. Moreover, it is assumed that the desired activity time is known by the scheduler. To motivate the above assumptions, the use-case for the washing machine is described (similar considerations can be applied to other considered ET loads).

Once the user have selected the type of washing cycle, the duration of the whole process is defined and can be made available to the controller. Moreover, the user can

explicitly select the desired completion time of the washing, i.e., the deadline. Nowadays, the current mode of employment of a washing machine allows the user to specify a delay before the starting of the washing process. We instead foresee the possibility to allow the user to specify a deadline, i.e., the time at which the laundry requires to be completed.

The utilization $U_i$ of a load, in this case, is defined as $U_i = C_i/D_i$[1]. From the utilization viewpoint, a ET load can be seen as a TT load with period equal to the relative deadline.

### *4.2. Peak load reduction*

The proposed coordination scheme is based on the Earliest Deadline First (EDF) scheduling algorithm for uniprocessors [38]. EDF assigns the highest priority to the load having the earliest absolute deadline among all loads that have a pending requested activation. EDF is widely recognized as the best real-time scheduling algorithm for uniprocessors. Together with the Rate Monotonic (RM) scheduling policy, it is an optimal algorithm. In other words, it is able to successfully schedule a load set if a feasible schedule exists. However, as proved in [39], EDF has better performance. Considering the applications discussed in this paper, the most relevant features of EDF when compared to RM are:

- the possibility to guarantee the schedule of load sets having higher utilization;
- for a given load set, it produces a lower number of preemptions;

An example of schedule of 4 loads generated by EDF is depicted in Figure 8. The real-time scheduling algorithm ensures that *only one load is active at any given time*. This feature automatically achieves the minimization of the peak load, which corresponds to the power absorption of the most power-consuming load.

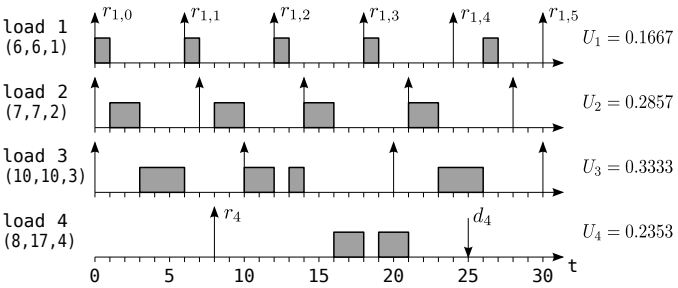


Figure 8: Example of schedule of 4 loads generated by EDF. Loads 1, 2 and 3 are TT, while load 4 is ET. Up arrows represent request times, while the down arrow is the absolute deadline. Absolute deadlines of TT loads are not shown, since they overlap with request times. The total utilization is $U = 0.9878$.

A relevant feature of the analysis of periodic real-time systems is the so-called *schedulability test*. The schedulability test is a condition that, if satisfied, ensures that the considered scheduling algorithm is able to generate a *valid schedule*. A schedule is said to be valid when the deadlines of every load are met, i.e., each load is activated for $C_i$ time units in the $[r_{i,k}, r_{i,k} + D_i]$. For TT loads, *implicit deadlines* are considered, i.e., $D_i = T_i$. Therefore, for the $i$-th load, the $k$-th absolute deadline corresponding to the $r_{i,k}$ request time is $d_{i,k} = r_{i,k} + T_i$. In case of implicit deadlines, the schedulability test for the uniprocessor EDF is $U^{tot} \leq 1$. This means that EDF is able to successfully schedule a task set if and only if the total utilization is less or equal to 100%.

The above schedulability test is valid in case of a full-preemptive model, i.e., where the scheduler is allowed to preempt an active load at any time.

#### *4.2.1. Load partitioning*

In realistic conditions, the set of loads may not be successfully schedulable by a uniprocessor real-time algorithm as EDF. This is detectable by applying the schedulability test. In the case of EDF, when the total utilization is

[1]This formulation of the utilization is sometimes referred as *density* in the real-time parlance.

greater than 1 the load set is not schedulable. A high utilization can be due to the large number of loads or due to high utilizations of single loads. In these conditions, a strategy is needed to deal with load sets having an utilization higher than the limit imposed by the schedulability test.

In [7], a load partitioning scheme is presented for this purpose. The referred method uses a two-dimensional level packing scheme to automatically organize the set of loads into a set of $m$ partitions $(\Omega_1, \ldots, \Omega_m)$, called *scheduling groups*. Each load is assigned to one scheduling group. Based on timing parameters of the load set derived from the physical model, it works by ordering the loads by decreasing power. Starting from the most power-consuming load, each load is added to an existing group if it schedulable by EDF in that group. Otherwise, a new scheduling group is created. This policy implements an allocation heuristic known as First-Fit Decreasing Height (FFDH) [40]. Such a method ensures that the total utilization of each scheduling group satisfies the schedulability test in that group, i.e. $U_{\Omega_i}^{\text{tot}} \leq 100\%$. In this way, the EDF algorithm can be applied independently to each group. The FFDH policy is conceived to generate a low number of scheduling groups, by packing the most power-consuming loads within the same scheduling groups. Since at most one load can be active at any given time in each scheduling group, such an assignment allows to limit the overall peak load of power consumption. The peak load is generated when the loads having the highest power consumption are simultaneously activated in all the scheduling groups. Figure 8 shows an example of the described behavior. Notice that the bi-dimensional packing problem has NP-hard complexity. The FFDH heuristic is an approximation having linear complexity. Its performance w.r.t. the optimal partitioning is discussed in [7] and [40].

It is worth to notice that this approach does not bring the the minimum achievable peak load, since the activation of loads belonging to different scheduling groups is not coordinated. However, the method has linear complexity, thus it can be suitably applied to large load sets. Moreover, its performance degradation with respect to the optimal allocation of loads is bounded [41].

### *4.3. Limiting preemptions*

The use of EDF as a scheduling algorithm to manage the loads in each scheduling group and – in particular – the possibility to use the utilization-based schedulability test, implicitly assumes a *full-preemptive system*. However, the full-preemtion may be dangerous when electric motors are involved. In fact, preemptions may cause frequent activations/deactivations of the motor, and may quickly damage the motor insulators and break the component. Therefore, while preemptions are needed to allow the proper operation of the scheduling algorithm, they should be limited to extend the system lifetime. Moreover, some loads are not fully preemptable due to their peculiar working cycle. For example, some stages of the washing machine working cycle do not well tolerate an interruption. As a consequence of above observations, it is necessary to limit the number of activations of each load to ensure its correct functionality and preserve the system lifetime.

In the field of real-time systems, the so-called *limited-preemption* model has been proposed in [42]. The limited-preemption EDF algorithm permits preemption where necessary for achieving the schedulability, but attempts to avoid unnecessary preemptions. This is done by determining, for each task in the system, the longest amount of time – namely, the non-preemption chunk $b_i$ – for which the task may execute non-preemptively without compromising the system schedulability.

A simple iterative algorithm to find $b_i$ values given the load set parameters is provided in [42]. The referred algorithm is applied in this paper to determine the value of $b_i$ for each load.

While the limited preemption approach is effective to limit the frequency of load activations, its original goal

is to improve the management of critical sections in real-time tasks, i.e., time intervals that must not be preempted. Therefore, it can be leveraged to manage loads usually considered non-preemptable, e.g., dish washers, washing machines and ovens. Since a non-preemption chunk can be placed anywhere during the load activity time, non-preemptive intervals of a load activation can be transparently managed if they fit within a chunk. The challenge becomes a system design problem, where suitable values of timing paramenters need to be found to obtain non-preemption chunks large enough.

## 5. User characterization

In order to assess the performance of the proposed HEM, it is necessary to characterize the users' behavior. In particular, realistic patterns of request times are required for ET loads. For this purpose, Table 2 has been derived from [12], which lists the usage probability of each ET load within a day.

The activation pattern of each ET load has been generated using the following algorithm. Time is discretized in slots of two hours. For each time slot, a random number in the range $[0, 100]$ is generated (uniform distribution); if such number is lower than the corresponding usage probability in Table 2, then the load is considered activated by the user, else the load is held off. Note that the loads are always triggered at the beginning of their time slot of activation. Such a choice allows to consider the worst-case condition in which loads with request time falling into the same slot are activated at the same instant.

After an extended set of simulations of activation patterns, two activation patterns have been identified as the most interesting to test the HEM strategy: the one having the highest probability, and the one leading to the worst-case situation. Such conditions are described in the reminder of this section.

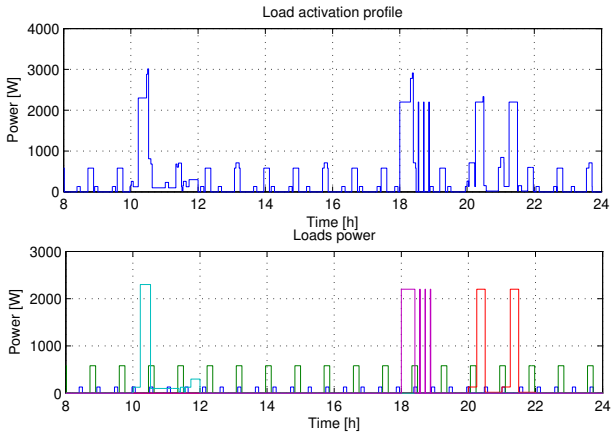


Figure 9: Absorption power profile generated by the typical activation pattern.

### 5.1. Typical activation pattern

This pattern represents the set of activations that appears more frequently in the simulations. In this case, each load is turned on in the interval of the maximum usage probability reported in Table 3.

Figure 9 shows the power profile corresponding to this pattern. At time $t = 0$ all TT loads are considered active, while the request time of the ET loads is chosen in accordance with Table 3. The bottom chart of Figure 9 shows that the maximum absorption power is 3012 W and it is due to the simultaneous activation of refrigerator, HVAC load and washing machine at about 10:30.

### 5.2. Worst activation sequence

This sequence produces the most power-intensive activation profile. All ET loads are activated at the same time at 18:00, see Table 3. The maximum peak power is equal to 7412 W. It is due to the simultaneous activation of electric oven, dishwasher, washing machine, refrigerator and space cooling, as depicted in Figure 10.

## 6. Example of application

This section describes the results of the application of the proposed algorithm to an example scenario where an

| Loads | 24-02 | 02-04 | 04-06 | 06-08 | 08-10 | 10-12 | 12-14 | 14-16 | 16-18 | 18-20 | 20-22 | 22-24 |
|---|---|---|---|---|---|---|---|---|---|---|---|---|
| Electric oven | 0% | 0% | 0% | 2% | 4% | 14% | 28% | 2% | 12% | 34% | 4% | 0% |
| Washing machine | 1% | 1% | 2% | 9% | 15% | 21% | 11% | 9% | 11% | 9% | 9% | 2% |
| Dishwasher | 1% | 1% | 1% | 3% | 8% | 8% | 3% | 12% | 0% | 15% | 36% | 12% |

Table 2: Usage probability for the considered ET load during a day. Time is discretized in two hours slots.

| Load | Power [W] | MP activation time [h] | W activation time [h] |
|---|---|---|---|
| WM | 2300 | 10:00 | 18:00 |
| EO | 2200 | 18:00 | 18:00 |
| DW | 2200 | 20:00 | 18:00 |

Table 3: represent the most probable (MP) and the worst (W) activation sequences for the chosen ET loads.

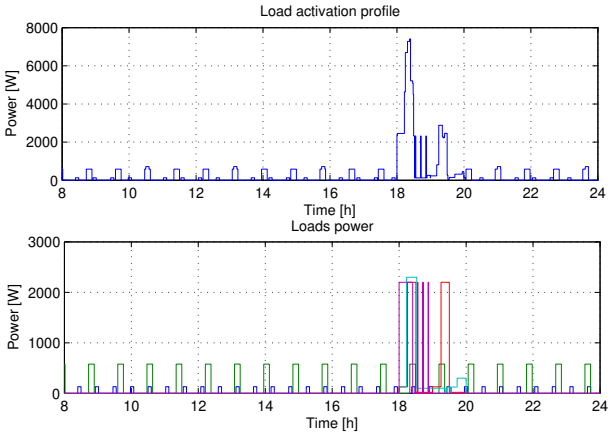


Figure 10: Absorption power profile generated by the worst activation sequence.

apartment is equipped with all the considered household appliances.

The control scheme works as follows. Once the value of timing parameters have been derived as shown Section 6.1, the load management is carried on automatically. First, the load set is partitioned using the heuristic described in Section 4.2.1. At run-time, the EDF algorithm schedules the activation of loads according to their timing parameters. Notice that scheduling decisions actually consist in the dynamic assignment of priorities to the loads. Based on this assignment, the scheduler dynamically activates

| Load | T [s] | C [s] | D [s] | U |
|---|---|---|---|---|
| Refrigerator | 1890.4 | 347.6 | $D \equiv T$ | 0.184 |
| HVAC | 3140.2 | 605.6 | $D \equiv T$ | 0.193 |
| Washing machine | n.a. | 7200.0 | 21600.0 | 0.333 |
| Dishwasher | n.a. | 7200.0 | 21600.0 | 0.333 |
| Electric oven | n.a. | 3600.0 | 4500.0 | 0.8 |

Table 4: Timing parameters of the considered loads (n.a. means "not applicable").

the highest priority load in each scheduling group. This task is automatically carried out by the scheduler itself.

### *6.1. From physical to timing parameters*

In the ideal case, i.e., without considering the effect of modeling errors, according to the physical model presented in Section 3.1, the slopes of the refrigerator temperature are respectively $\alpha^{\text{on}} = 10.357$ °C/hour and $\alpha^{\text{off}} = 2.333$°C/h, whereas the HVAC system has a decreasing slope $\alpha^{\text{on}} = 2.97$ °C/h and a increasing slope $\alpha^{\text{off}} = 0.71$ °C/h. Based on these vales, (14) is applied to derive the values of real-time parameters for the refrigerator and the HVAC unit, which are reported in Table 4.

It is worth to note that, in case of uncertainties, the activation time value may change in each time frame, according to (15).

The refrigerator and the HVAC have a relatively low utilization. This is an important feature, since it enables the concurrent management of many loads while achieving the quality of service required by each of them.

The evaluation of the contribution to the overall utiliza-

tion due to ET loads requires to consider a use-case scenario to determine the value of real-time parameters. In the simulation example, the washing machine has a washing cycle of 2 hours and a relative deadline of $D_{\mathrm{WM}} = 6$ hours. Therefore the utilization is $U_{\mathrm{WM}} = 0.33$. The profile of temperature variation and power absorption is shown in Figure 4. Same values are used for the washing cycle duration $C_{\mathrm{DW}}$ of the dishwasher and its relative deadline $D_{\mathrm{DW}}$, bringing to the same utilization. Its load profile is depicted in Figure 5. Finally, the cooking cycle of the electric oven has a duration $C_{\mathrm{EO}} = 1$ hour and a short relative deadline $D_{\mathrm{EO}} = 75$ minutes, which determines an high utilization $U_{\mathrm{EO}} = 0.8$. The selection of a short relative deadline reflects the scarce willingness of the user to tolerate delays in the cooking process.

Despite the load profiles shown in Figures 4 to 6, in this example it is made the pessimistic assumption that the ET loads consumes the whole amount of power during all their working time. While this assumption produce a worst-case load profile, it helps to depict the contribution of each load in the overall load profile. Moreover, it does not affect the behavior of the scheduler, which is only based on timing parameters reported in Table 4.

Given the utilization of each load, the overall utilization is $U_{tot} = 1.843 > 1$. It follows that simultaneous activations can not be completely avoided by the uniprocessor EDF. Therefore, it is necessary to partition the set of loads using the method explained in Section 4.2.1.

According to the partitioning scheme, two scheduling groups have been generated. Table 5 shows the assignment of loads to the partitions, together with the relevant related information.

The washing machine, the dishwasher and the HVAC system are assigned to the $\Omega_1$ scheduling group. The total utilization of this group is equal to $0.859 \leq 1$, thus the loads are successfully schedulable by EDF. The peak load is equal to 2300 W. It is due to the washing machine, the most power-consuming load. The $\Omega_2$ scheduling group manages the electric oven and the refrigerator, for a total utilization equal to 0.984. The peak load is 2200 W, which is associated to the electric oven.

| Sched. group | Load | $P$ [W] | $U$ | $U^{\mathrm{tot}}$ | $P^{\max}$ |
|---|---|---|---|---|---|
| $\Omega_1$ | Wash. m. | 2300 | 0.33 | 0.86 | 2300 |
| | Dishw. | 2200 | 0.33 | | |
| | HVAC | 580 | 0.19 | | |
| $\Omega_2$ | Oven | 2200 | 0.80 | 0.98 | 2200 |
| | Refrig. | 132 | 0.18 | | |

Table 5: Utilization and power absorption for each considered load. Loads are grouped to show the two generated scheduling groups $\Omega_1$ and $\Omega_2$. The total utilization and the highest possible power consumption is shown for the two scheduling groups in the latest two columns.

As a consequence of the applied partitioning, the use of EDF to coordinate the activation of loads in each scheduling group ensures that only one load is active at any given time in each scheduling group. Therefore, the theoretical overall peak load is obtained when the most power-consuming loads are activated simultaneously in all the scheduling groups. This condition represents the worst case situation in the partitioned scenario. According to this observation, the maximum possible peak load power is $P^{\max} = P^{\max}_{\Omega_1} + P^{\max}_{\Omega_2} = 4500$ W. Without automatic coordination, the highest theoretical peak load is equal to the sum of all loads power, i.e. $P^{\max} = 7412$ W. Therefore, in this case, the proposed load scheduling approach reduces the theoretical peak load up to 40%. Table 6 reports the non-preemptive chunks $b_i$ for every loads, calculated as described in section 4.3.

### *6.2. Quantitative results*

This section describes the results obtained in the application of the proposed control scheme to the example load set adopted in Section 6.1. Release times of ET loads

| Scheduling group 1 | | Scheduling group 2 | |
|---|---|---|---|
| Load | $b_i$ [s] | Load | $b_i$ [s] |
| Dishwasher | 2534 | Electric oven | 1542 |
| Washing machine | 2534 | Fridge | 348 |
| Air conditioning | 606 | - | - |

Table 6: Non-preemptive chunks for each load.

follow the two activation patterns derived in Sections 5.1 and 5.2.

Figure 11a shows the absorption power profile obtained by scheduling the load set when the typical activation pattern is applied, while Figure 11b depicts the profile with no control actions in the same conditions.

Focusing on Figure 11b it can be noted that the peak load occurs in the interval from 10:00 to 12:00 and it is due to the simultaneous activation of fridge, air conditioning and washing machine. The comparison of Figure 11a and Figure 11b shows that using the proposed scheduling algorithm the peak load is shaved. In particular, a peak power reduction of 20% is achieved. The reduction is obtained by preempting the working cycle of the dishwasher and shifting the activation of the HVAC system from the beginning to the end of its period. The comparison between the top of Fig. 11a and Fig. 11b makes this effect clear. As reported in Figure 12, the shifted activation of the air conditioner does not cause the room temperature to exceed the desired bounds.

The scheduler shifts the peak load from 10:00 to about 18:30, when only the air conditioning and the electric oven are activated. Therefore, considering the probable sequence of activation, the maximum power amounts to 2780 W, ensuring a reduction of the peak load of about 8%.

Similar considerations can be done for the worst activation sequence described in Section 5.2. According to that activation sequence, without scheduler control all the ET loads are triggered simultaneously at 18:00. This fact determines a peak load of 7412 W, as depicted in Figure 13b. The HEM activation pattern is plotted in Figure 13a. The figure shows that the scheduler is not able to prevent the simultaneous activation of the electric oven and the washing machine. In fact, as explained in Section 4.2.1, the partitioning scheme can only avoid the simultaneous activation of loads belonging to the same scheduling group. According to this behavior, the washing machine, the dishwasher and air conditioner are never activated simultaneously in the first scheduling group. This is achieved by performing the following actions: the activation of the air conditioner is shifted from the beginning to the end of its period at 18:00; the activation of refrigerator is scheduled at 18:30; the dishwasher activation is shifted from 18:00 to 20:20, when the washing machine complete its working cycle; finally, the dishwasher and the washing machine are preempted when necessary. In conclusion, the scheduler is able to reduce the peak load, in the worst case activation sequence, of about 41%: from 7412 W to 4400 W.

## 7. Multi-user scenario

This section evaluates the benefits of the proposed HEM when the users adopt a coalitional approach [10]. A *coalition* is a set of users, e.g., the inhabitants of the same building, which adopt the load shifting strategy as a unitary *Virtual Electricity Consumer* (VEC). This multi-user scenario is provided to exhibit the scalability potential of the proposed method. On the other hand, we have limited the number of coordinated apartments to 5 to simplify the presentation.

The simulation set considers a building composed by 5 identical apartments. Each apartment is provided with 5 electric appliances. Apartments are denoted with letters from $A$ to $E$. The appliances have been divided into TT and ET loads, according to the definition given in Section 3. Air-conditioning systems (ac) and fridges (fr) are classified as TT loads and we consider washing machine

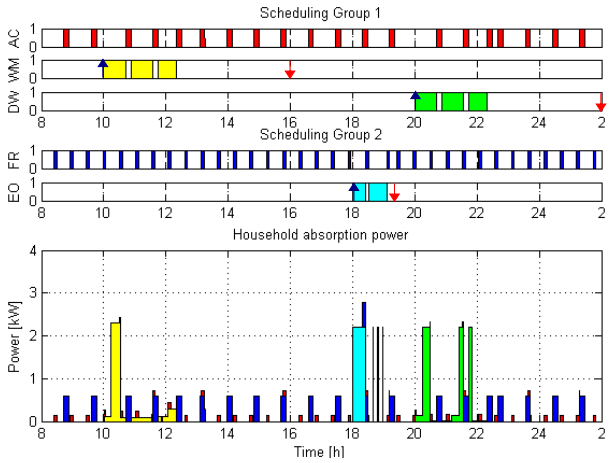


(a) With scheduling actions.

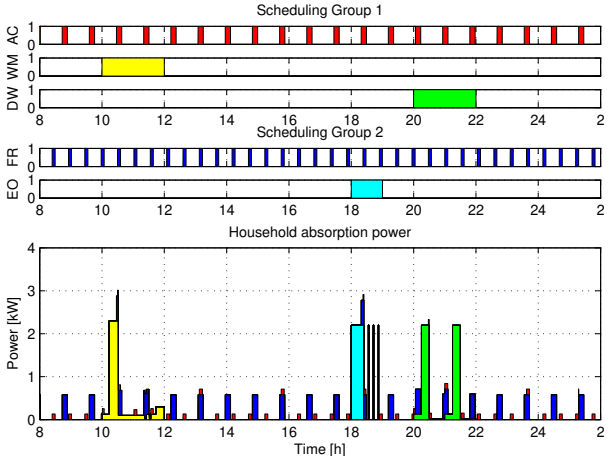


(b) Without scheduling actions.

Figure 11: Activation sequence and power absorption profile of loads in one apartment in the most probable case.

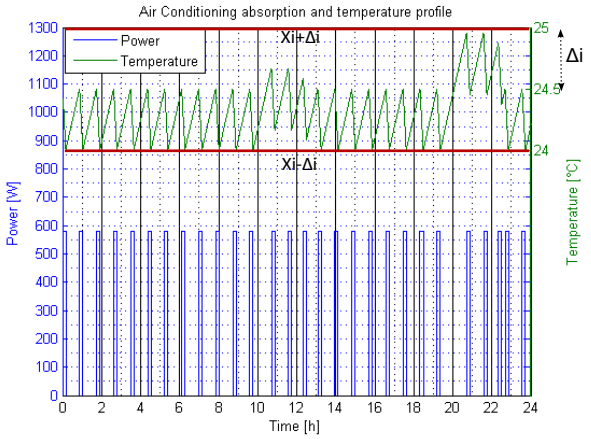


Figure 12: Most probable power absorption profile of an air conditioner during one typical day. The controlled temperature remains within the desired interval even during intense scheduling actions happening in the time frame $[20, 23]$h.

(WM), dishwasher (DW) and electric oven (EO) as ET loads. Each appliance is identified by its type and the apartment which belong to. The adopted notation is $X_{\text{app}}$, where $X$ is the apartment identifier and *app* is the appliance. For instance, the washing machine of apartment $A$ is indicated as $A_{\text{WM}}$. In the coalitional scenario, the scheduler considers the 5 apartments as a unique virtual apartment.

To evaluate the performance of the scheduling approach under the coalitional scenario, an extended set of simulations has been carried out. The simulations can be divided into two different cases: a typical and a worst case. Details of each considered case are reported in the following sections. In both cases, the set of loads in the virtual apartment is partitioned using the rules described in Section 4.2.1. The load set is composed by 25 loads, so the total utilization is about $9.22 > 1$. Therefore, it is necessary to partition the loads into 10 distinct scheduling groups, $\Omega_{1\ldots10}$. Table 7 shows the obtained scheduling groups. For each group, its utilization, the maximum peak power and the assigned loads are indicated.

Considering this organization of scheduling groups, the results in typical and worst cases are now illustrated.

### *7.1. Typical activation sequence*

To statistically evaluate the performance of the scheduling approach in the typical case, a total amount of 1000 different activation patterns have been generated according to the usage probabilities reported in Table 2. Patterns in this simulation thus include the activation sequences that occur with higher probabilities. The distribution of peak loads associated with the activation sequences in the

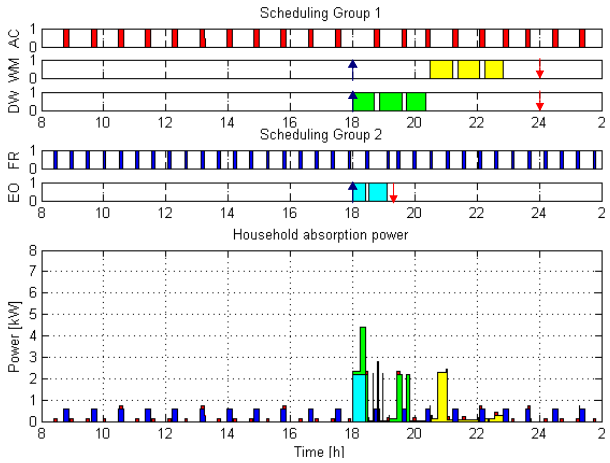


(a) With scheduling actions.

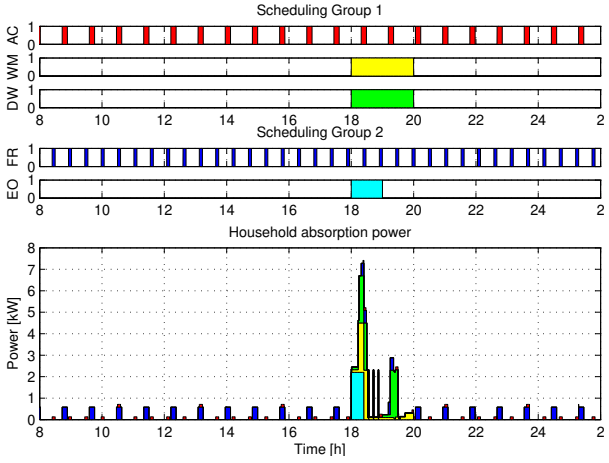


(b) Without scheduling actions.

Figure 13: Activation sequence and power absorption profile of loads in one apartment in the worst case.

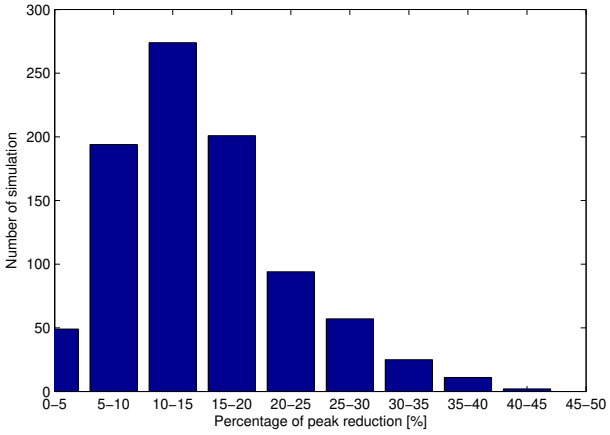


Figure 14: Frequency of peak power reduction percentage w.r.t. the absence of coordination, shown for range of of 5%.

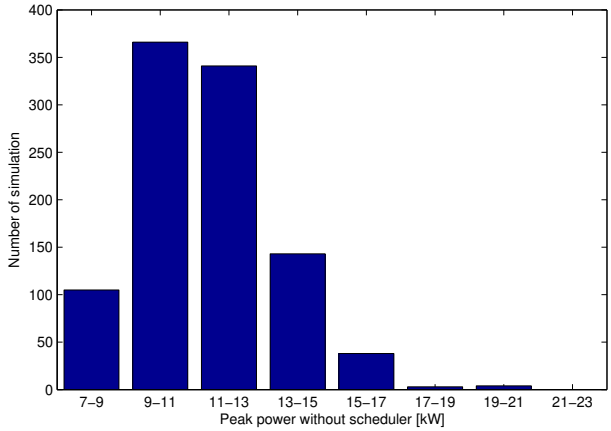


Figure 15: Peak power frequency without scheduler's coordination, in power range of 2 kW.

simulation allows to identify the most frequent peak power absorption.

First, we present in Figure 14 the distribution of the peak power reduction obtained by the VEC scheduler coordination w.r.t. the absence of coordination. Each bar depicts the number of simulations that produced a peak load reduction in the corresponding range of power level. The graph shows that the typical peak load reduction is in the range $10-15\%$. This happens in more than 250 cases. In particular, the average peak load reduction is 14.97%.

To better understand the behavior of the scheduler in the VEC scenario, we also report the frequency of the peak power obtained in the simulation. The distribution reported in Figure 15 shows that the most frequent peak load is in the range between $9-11$ kW. In particular, without scheduler coordination, the most common peak value is 10.16 kW. The sequence in Table 8 is an example of those patterns that generates the most frequent peak load.

The application of the proposed control algorithm to the simulation setup brings to the power absorption pro-

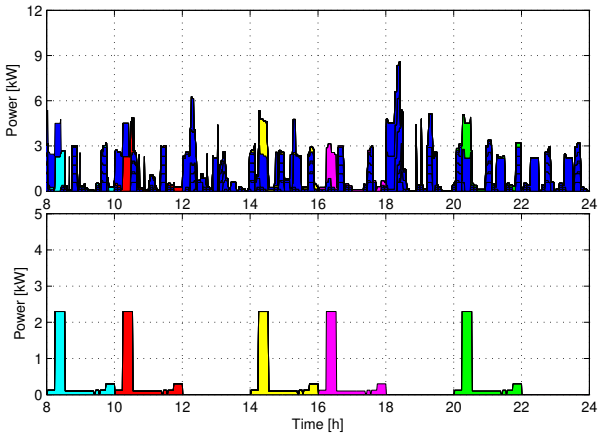


(a) Washing machines activation sequence.

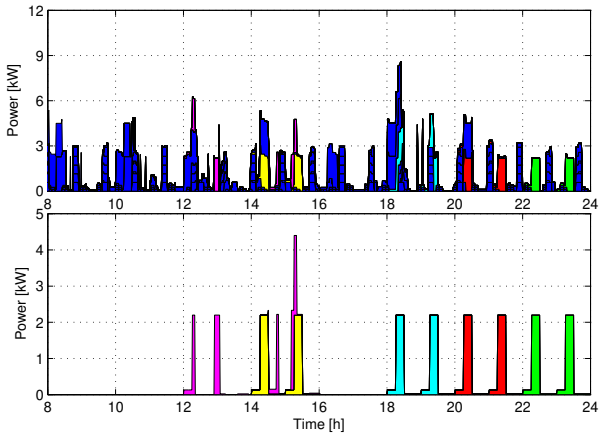


(b) Dishwashers activation sequence.

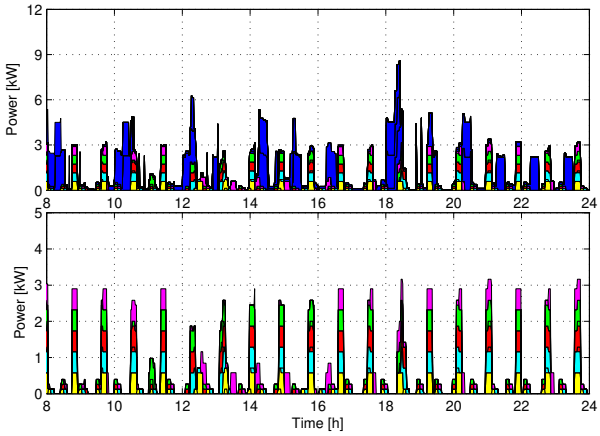


(c) Activation sequence of TT loads.

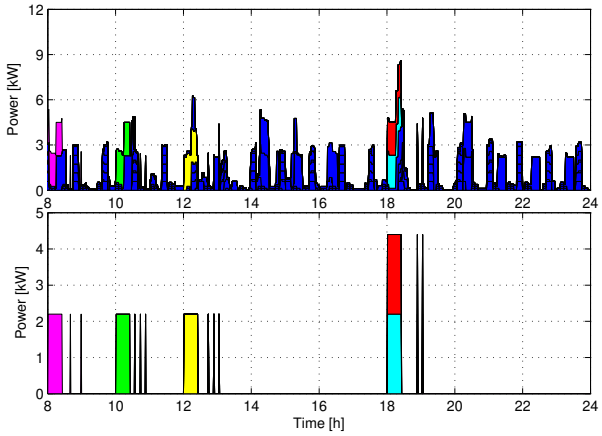


(d) Electric ovens activation sequence.

Figure 16: Building load profile for each type of load and each apartment in the typical case. Loads in each apartment are identified by colors: A – yellow; B – light blue; C – red; D – violet; E – green.

file shown in Figure 16. The figures show the contribution of each load to the total load absorption profile. For instance, the washing machine load profiles are described in Figure 16a. Each chart shows, on the bottom, the power profile of each load, in its interval of activation. Its effect on the total absorption profile is instead depicted in top charts.

Focusing on the top chart of Figure 16a, a peak of 8.6 kW can be distinguished in the interval from 18:00 to 20:00. The peak load is due to the simultaneous activation of $B_{EO}$, the light blue one, $C_{EO}$, the red one (Figure 16d) and $B_{WM}$ (Figure 16a). This condition brings to a power consumption of 6.7 kW, which significantly contributes to the peak load of 8.6 kW.

### *7.2. Worst activation sequence*

In the VEC scenario, the worst-case activation sequence takes place when the activations of all the ET loads are triggered at 18:00 in every apartment. Figure 17 shows the results of the application of the proposed scheduling algorithm to the worst case. The top chart of Figure 17d shows that the worst peak load occurs from 18:00 to 20:00. In this time interval, as depicted in the bottom chart of Figure 17d, all the electric ovens are simultaneously activated. This leads to the peak load condition, where the

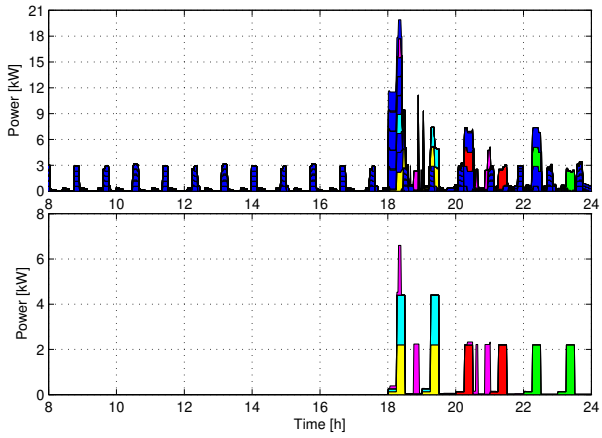


(a) Washing machines activation sequence.

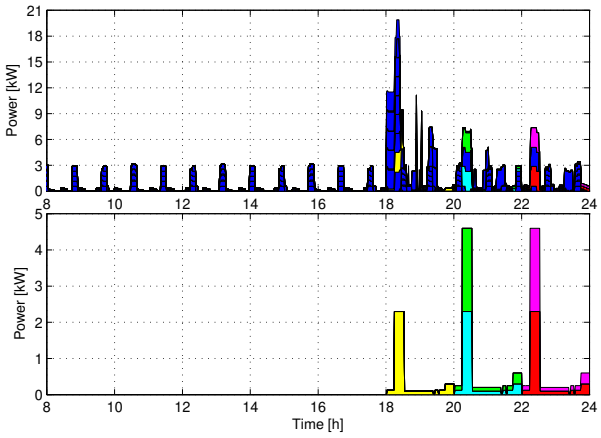


(b) Dishwashers activation sequence.

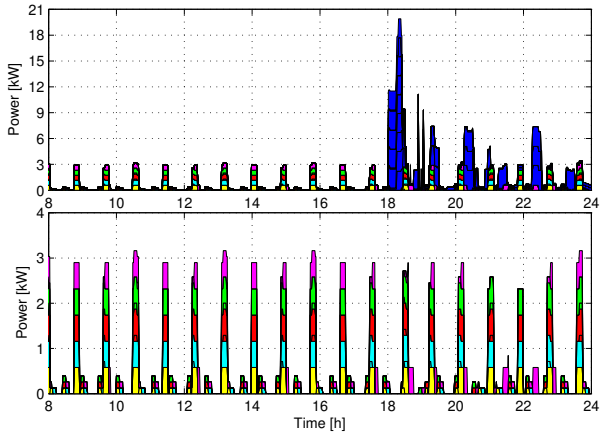


(c) Activation sequence of TT loads.

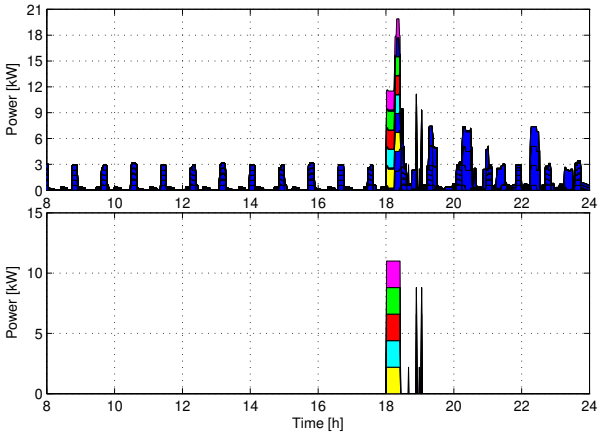


(d) Electric ovens activation sequence.

Figure 17: Building load profile for each type of load and each apartment in the worst case. Loads in each apartment are identified by colors: A – yellow; B – light blue; C – red; D – violet; E – green.

power consumed by the ovens represents the 55% of the total peak power. This condition of simultaneous activation can not be avoided. In fact, due to the high utilization of ovens, the partitioning scheme places each oven in a different scheduling group (see Table 7). Since the load activation is not coordinated among different scheduling groups, the scheduler can not avoid the simultaneous activation of ovens.

### *7.3. Comparison between cases*

Given the results described in previous sections, we provide some observations concerning the comparison between the different considered scenarios.

Table 9 shows the peak power obtained with the proposed coordination strategies (absence of coordination, per-apartment scheduling and VEC scheduling) in three different cases: theoretical, typical and worst-case. The typical and worst-case scenarios are those analyzed in Section 7.1 and Section 7.3, respectively. The theoretical peak load represents the sum of the power required by most power-consuming loads in all the scheduling groups. Instead, in absence of scheduling actions, the theoretical peak load corresponds to the sum of the power consumed by all the loads. Although this condition may happen rather rarely, we consider it as a reference condition for

| Sched. group | Loads | $U$ | $P$ [W] |
|---|---|---|---|
| $\Omega_1$ | $\{A_{WM}, B_{WM}, C_{WM}\}$ | 1 | 2300 |
| $\Omega_2$ | $\{A_{DW}, D_{WM}, E_{WM}\}$ | 1 | 2300 |
| $\Omega_3$ | $\{A_{EO}, A_{ac}\}$ | 0.992 | 2200 |
| $\Omega_4$ | $\{B_{DW}, C_{DW}, D_{DW}\}$ | 1 | 2200 |
| $\Omega_5$ | $\{B_{EO}, B_{ac}\}$ | 0.992 | 2200 |
| $\Omega_6$ | $\{C_{EO}, C_{ac}\}$ | 0.992 | 2200 |
| $\Omega_7$ | $\{D_{EO}, D_{ac}\}$ | 0.992 | 2200 |
| $\Omega_8$ | $\{A_{fr}, B_{fr}, E_{ac}, E_{DW}\}$ | 1 | 2200 |
| $\Omega_9$ | $\{C_{fr}, E_{EO}\}$ | 0.992 | 2200 |
| $\Omega_{10}$ | $\{D_{fr}, F_{fr}\}$ | 0.368 | 132 |

Table 7: Utilization and power absorption for each considered load set. Loads are grouped to show the ten generated scheduling groups $\Omega_{1...10}$. The total utilization and the highest possible power consumption is shown for the two scheduling groups in the latest two columns.

comparison purposes.

As expected, every peak load in worst-case conditions is very close or equal to the theoretical peak load. The scheduling of VEC loads leads to better results than the per-apartment scheduling, which in turn has better performance than the absence of coordination. The application of the scheduling policy to each apartment independently, i.e., without the users' coalition, achieves a peak load of 22.5 kW. Therefore, the coalitional approach ensures an improvement in terms of peak load reduction of about the 11% w.r.t. the single apartment scheduling.

In some specific simulations concerning the comparison between the VEC scenario and the absence of coordination, significant peak load reductions have been measured. In particular, a reduction up to 15% (from 10.16 to 8.6 kW) and up to 46% (from 37.06 to 20.03 kW) were registered in the typical and worst case, respectively. Two examples of load profiles that produce such behaviors are depicted in Figure 18.

## 8. Conclusion

This paper presented a technique for the Electric Load Management based on real-time scheduling. The goal has been the peak load reduction together with the achievement of service constraints on the controlled loads. To assess the performance of the scheduling approach, the method has been applied a properly modeled set of household appliances. A combination of a level packing strategy, limited preemption scheme and a careful selection of timing parameters allowed to meet both timing and service constraints. Simulations on a single apartment proved the possibility to use the proposed techniques in realistic use cases. In this case, the peak load is reduced by the 8% in the average case and by the 41% w.r.t. the worst-case. The benefits improve in case of coalitions, i.e., when the scheduler can manage a set of apartments as a unitary Virtual Electricity Consumer. Considering the coalition of several apartments, the scheduling approach achieves a peak load reduction up to 46%.

## References


[1] C. Gellings, Then and now: The perspective of the man who coined the term 'dsm', Energy Policy 24 (4) (1996) 285–288.

[2] P. Palensky, D. Dietrich, Demand side management: Demand response, intelligent energy systems, and smart loads, IEEE Transactions on Industrial Informatics 7 (3) (2011) 381–388.

[3] G. Buttazzo, Hard Real-Time Computing Systems: Predictable Scheduling Algorithms and Applications, Springer, 2011.

[4] T. Facchinetti, M. L. Della Vedova, Real-time modeling for direct load control in cyber-physical power systems, IEEE Transactions on Industrial Informatics, special issue on Information Technology in Automation 7 (4) (2011) 689–698.

[5] T. Facchinetti, The many faces of real-time scheduling applied to power load management, in: Proceedings of the Third International Conference on Smart Grids, Green Communications and IT Energy-aware Technologies (Energy), 2013.

[6] M. L. Della Vedova, E. Di Palma, T. Facchinetti, Electric loads as real-time tasks: an application of real-time physical systems, in: 7th International Wireless Communications and Mobile Computing Conference (IWCMC), 2011, pp. 1117–1123.

[7] M. L. Della Vedova, T. Facchinetti, Real-time scheduling for peak load reduction in a large set of hvac loads, in: Proceedings

| Load | 24-08 | 08-10 | 10-12 | 12-14 | 14-16 | 16-18 | 18-20 | 20-22 | 22-24 |
|---|---|---|---|---|---|---|---|---|---|
| EO | - | $E$ | $D$ | $A$ | - | $B, C$ | - | - | |
| WM | - | $B$ | $C$ | - | $A$ | $E$ | - | $D$ | - |
| DW | - | - | - | $E$ | $A$ | - | $B$ | $C, D$ | - |

Table 8: Activation of ET loads in the multi-user scenario.

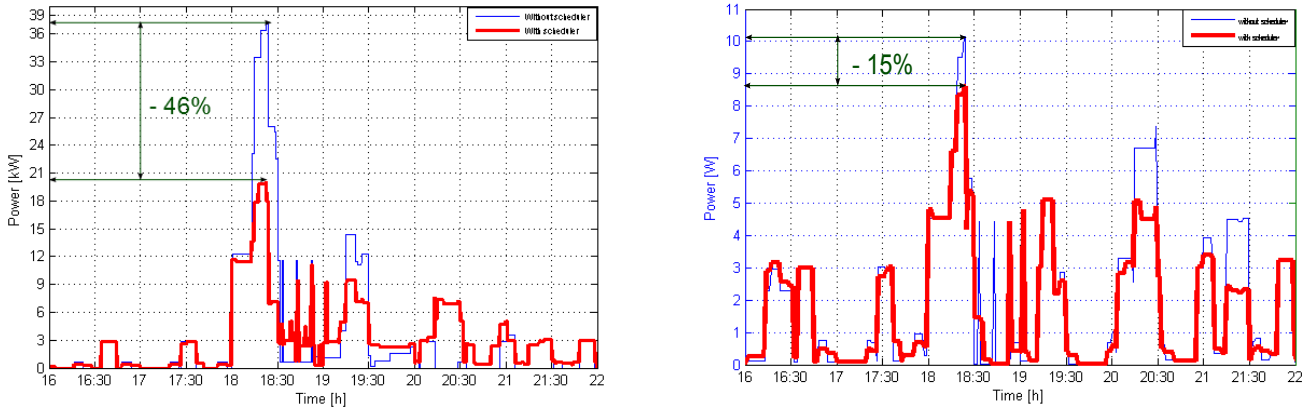


(a) Worst case load profile during the time interval corresponding to the peak load.

(b) Typical load profile during the time interval corresponding to the peak load.

Figure 18: Comparison between power absorption profiles with or without scheduler in each case.

| Use case | Theor. [kW] | Typical [kW] | Worst [kW] |
|---|---|---|---|
| No sched. | 37.06 | 10.16 | 37.06 |
| Single sched. | 22.50 | 9.39 | 22.00 |
| VEC sched. | 20.13 | 8.60 | 20.03 |

Table 9: Peak power demand registered of 5 apartments under the considered simulation scenarios: absence of scheduling actions, independent scheduling of each apartment (single sched.), coordinated scheduling of all the apartments in the coalition (VEC sched.).


of the Third International Conference on Smart Grids, Green Communications and IT Energy-aware Technologies (Energy), 2013.

[8] M. L. Della Vedova, T. Facchinetti, Real-time scheduling for industrial load management, in: Proceeding of the 2nd ENERGYCON Conference & Exhibition, 2012.

[9] G. Quartarone, N. Anglani, T. Facchinetti, Improving energy management of electrically driven air compressors through real-time scheduling techniques, in: Proceedings of the 37th Annual Conference of the IEEE Industrial Electronics Society (IECON), 2011, pp. 2697–2702.

[10] M. Vinyals, F. Bistaffa, A. Farinelli, A. Rogers, Coalitional energy purchasing in the smart grid, in: Energy Conference and Exhibition (ENERGYCON), 2012 IEEE International, 2012, pp. 848 –853.

[11] Inchiesta su caratteristiche e utilizzo degli elettrodomestici del freddo, del lavaggio e della cottura da parte degli utenti finali, Tech. rep., ENEA – Agenzia Nazionale per le nuove tecnologie, l'energia e lo sviluppo economico sostenibile (2011).

[12] Evaluation of environmental benefits, reduction of $co_2$ emissions, added value for new buildings due to application of energy management functions through connected appliances, Tech. rep., Department of Electrical, Electronic and Telecommunications Engineering, University of Palermo (Italy) (2007).

[13] J. H. Michael Rathmair, Simulator for smart load management in home appliances, 2012.

[14] A. Molina, A. Gabaldon, J. Fuentes, C. Alvarez, Implementation and assessment of physically based electrical load models: Application to direct load control residential programmes, Generation, Transmission and Distribution, IEE Proceedings 150 (1) (2003) 61–66.

[15] A. Gomes, C. Antunes, A. Martins, Physically-based load de-

mand models for assessing electric load control actions, in: PowerTech, 2009 IEEE Bucharest, 2009, pp. 1–8.

[16] T. Calloway, C. Brice, Physically-based model of demand with applications to load management assessment and load forecasting, Power Apparatus and Systems, IEEE Transactions on PAS-101 (12) (1982) 4625–4631.

[17] A. Di Giorgio, L. Pimpinella, An event driven smart home controller enabling consumer economic saving and automated demand side management, Applied Energy 96 (2012) 92–103.

[18] C. Babu, S. Ashok, Optimal utilization of renewable energy-based ipps for industrial load management, Renewable Energy 34 (11) (2009) 2455–2460.

[19] N. Padhy, S. Paranjothi, V. Ramachandran, A hybrid fuzzy neural network-expert system for a short term unit commitment problem, Microelectronics Reliability 37 (5) (1997) 733–737.

[20] M. Deindl, C. Block, R. Vahidov, D. Neumann, Load shifting agents for automated demand side management in micro energy grids, in: Proceedings - 2nd IEEE International Conference on Self-Adaptive and Self-Organizing Systems, SASO 2008, 2008, pp. 487–488.

[21] G. Tsekouras, P. Kotoulas, C. Tsirekis, E. Dialynas, N. Hatziargyriou, A pattern recognition methodology for evaluation of load profiles and typical days of large electricity customers, Electric Power Systems Research 78 (9) (2008) 1494–1510.

[22] H.-T. Yang, K.-Y. Huang, Direct load control using fuzzy dynamic programming, IEE Proceedings: Generation, Transmission and Distribution 146 (3) (1999) 294–300.

[23] J.-L. Chen, Y.-Y. Hsu, Expert system for load allocation in distribution expansion planning, IEEE Transactions on Power Delivery 4 (3) (1989) 1910–1918.

[24] J. Wang, C. Liu, D. Ton, Y. Zhou, J. Kim, A. Vyas, Impact of plug-in hybrid electric vehicles on power systems with demand response and wind power, Energy Policy 39 (7) (2011) 4016–4021.

[25] S. Gottwalt, W. Ketter, C. Block, J. Collins, C. Weinhardt, Demand side management-a simulation of household behavior under variable prices, Energy Policy 39 (12) (2011) 8163–8174.

[26] A. Molina-Garca, M. Kessler, J. Fuentes, E. Gmez-Lzaro, Probabilistic characterization of thermostatically controlled loads to model the impact of demand response programs, IEEE Transactions on Power Systems 26 (1) (2011) 241–251.

[27] T. X. Nghiem, M. Behl, R. Mangharam, G. J. Pappas, Green scheduling of control systems for peak demand reduction, in: IEEE Conference on Decision and Control and European Control Conference (CDC-ECC), 2011, pp. 5131–5136.

[28] S. Shao, M. Pipattanasomporn, S. Rahman, Development of physical-based demand response-enabled residential load models, Power Systems, IEEE Transactions on PP (99) (2012) 1.

[29] M. Pipattanasomporn, M. Kuzlu, S. Rahman, An algorithm for intelligent home energy management and demand response analysis, Smart Grid, IEEE Transactions on PP (99) (2012) 1.

[30] T. Facchinetti, M. L. Della Vedova, Real-time modeling and control of a cyber-physical energy system, in: Proceedings of the First International Workshop on Energy Aware Design and Analysis of Cyber Physical Systems (WEA-CPS), 2010.

[31] T. Facchinetti, E. Bini, M. Bertogna, Reducing the peak power through real-time scheduling techniques in cyber-physical energy systems, in: Proceedings of the First International Workshop on Energy Aware Design and Analysis of Cyber Physical Systems (WEA-CPS), 2010.

[32] M. Della Vedova, M. Ruggeri, T. Facchinetti, On real-time physical systems, in: Proceedings of the 18th International Conference on Real-Time and Network Systems (RTNS), 2010, pp. 41–49.

[33] M. L. Della Vedova, T. Facchinetti, Feedback scheduling of real-time physical systems with integrator dynamics, in: Proceedings of 17th IEEE International Conference on Emerging Technologies and Factory Automation (ETFA), 2012.

[34] D. Callaway, I. Hiskens, Achieving controllability of electric loads, Proceedings of the IEEE 99 (1) (2011) 184–199.

[35] B. Lu, M. Shahidehpour, Short-term scheduling of battery in a grid-connected pv/battery system, Power Systems, IEEE Transactions on 20 (2) (2005) 1053–1061.

[36] D. Maly, K. Kwan, Optimal battery energy storage system (BESS) charge scheduling with dynamic programming, Science, Measurement and Technology, IEE Proceedings 142 (6) (1995) 453–458.

[37] C. European Parliament, On the indication by labelling and standard product information of the consumption of energy and other resources by energy-related product, Official journal of the European Union.

[38] C. L. Liu, J. W. Layland, Scheduling algorithms for multiprogramming in a hard real-time environment, Journal of the Association for Computing Machinery 20 (1) (1973) 46–61.

[39] G. C. Buttazzo, Rate monotonic vs. EDF: Judgment day, in: Proceedings of the 3$^{rd}$ International Conference on Embedded Software, Philadelphia (PA), U.S.A., 2003, pp. 67–83.

[40] A. Lodi, S. Martello, M. Monaci, Two-dimensional packing problems: A survey, European Journal of Operational Research 141 (2) (2002) 241–252.

[41] A. Lodi, S. Martello, D. Vigo, Models and bounds for two-dimensional level packing problems, Journal of Combinatorial Optimization 8 (3) (2004) 363–379.

[42] S. Baruah, The limited-preemption uniprocessor scheduling of sporadic task systems, in: Proceedings of the Euromicro Conference on Real-Time Systems (ECRTS), 2005, pp. 137–144.